Geometric morphometrics and qualitative patterns in the morphological variation of five species of *Micrasterias* (*Zygnemophyceae*, *Viridiplantae*)

Geometrická morfometrika a kvalitativní vzorce morfologické variability u pěti druhů rodu *Micrasterias* (*Zygnemophyceae*, *Viridiplantae*)

Jiří Neustupa & Pavel Škaloud

Department of Botany, Faculty of Science, Charles University of Prague, Benátská 2, Praha 2, CZ-128 01, Czech Republic, e-mail: neustupa@natur.cuni.cz

Neustupa J. & Škaloud P. (2007): Geometric morphometrics and qualitative patterns of morphological variation in five species of *Micrasterias* (*Zygnematophyceae*, *Viridiplantae*). – Preslia 79: 401–417.

Geometric morphometric analyses were conducted on cultured populations of five *Micrasterias* species (*M. crux-melitensis*, *M. papillifera*, *M. rotata*, *M. thomasiana*, *M. truncata*). The patterns in the morphological variation measured using the morphospaces spanned by a PCA of morphometric data for individual populations were compared. In addition, the 18S rDNA sequences of these species are reported. The phenetic comparisons demonstrated the overall great similarity of morphometric indicators extracted from isolated polar lobe data and 18S rDNA genetic distances, and also indicated that the morphometric data of complete semicells were less well correlated with 18S rDNA distances. The phylogenetic analysis revealed clustering of the *Micrasterias* sequences into two clades, which correspond to qualitative patterns in the morphological variation of isolated polar lobe data. We propose that patterns of variation in the polar lobes of *Micrasterias* should be used in phenotype analyses of morphologically closely similar or cryptic species.

Keywords: *Desmidiales*, geometric morphometrics, *Micrasterias,* molecular phylogeny, morphological variation, *Streptophyta*

Introduction

Species of the genus *Micrasterias* C. Agardh ex Ralfs belong to one of the most conspicuous protists. Their elaborate cells have attracted the attention of botanists and protistologists since the early 19th century (Ralfs 1848). The genus consists of desmids with flattened, radiating cells composed of two semicells, each with a single polar lobe and two lateral dissected lobes (Prescott et al. 1977, for detailed description of *Micrasterias* morphology and terminology see e.g. Růžička 1981). The structure of the polar lobe was consistently considered as fundamental for infrageneric classification (Prescott et al. 1977, Růžička 1981).

More recently, different morphometric methods based on measurements of cells were used in taxonomic studies of this genus (Vyverman & Viane 1995, Gil-Gil & Bicudo 2000, Bicudo & Gil-Gil 2003). However, with the use of modern geometric morphometric tools in the shape analyses of protists (e.g. Haines & Crampton 2000, Quillevere et al. 2002, Beszteri et al. 2005, Neustupa & Hodač 2005), the application of these methods to elaborate desmid shapes has raised intriguing questions. Neustupa & Šťastný (2006) analysed geometric morphometric landmark-based data of semicells in natural samples of 14 Central European *Micrasterias* species. In accordance with traditional taxonomy, the spe-

cies investigated consistently clustered into two subgroups differing primarily in width of the polar lobe, which is associated with the depth of the incisions between lateral lobules. The first subgroup, characterized by a wide polar lobe, includes eight species including *Micrasterias truncata* and *M. crux-melitensis*. The second subgroup, characterized by a narrow polar lobe and deeply dissected lateral lobes, is composed of six species including *Micrasterias rotata*, *M. thomasiana* and *M. papillifera* (Neustupa & Šťastný 2006). Molecular phylogenetic analyses revealed the artificial status of numerous desmid genera (Gontcharov et al. 2003, Gontcharov & Melkonian 2005). However, there is still very little published information on the genus *Micrasterias*. The 18S rDNA phylogeny confirmed the position of the genus *Micrasterias* within the *Desmidiaceae*, but the reconstructions involved sequences from only two species (Gontcharov et al 2003).

In this study, the results of geometric morphometric analyses of shape variation in populations of five common *Micrasterias* species are reported. Parallel analyses of whole semicells and separated polar lobes were conducted to explicitly test the hypothesis that the structure of the polar lobe better discriminates between individual species populations than traditional experience-based taxonomy. Secondly, we used *Micrasterias* as a model group to demonstrate the applicability of qualitative indicators of morphological variation when comparing individual species populations. The qualitative patterns of variation in population samples (depicted as main axes of principal component analysis of morphometric data – PCA) were characterized to test the hypothesis that morphologically similar species share similar patterns of phenotypic variation. Species populations derived from a single cell and cultured in identical standard conditions were analysed. In such conditions, the morphological differences between individual adult cells within a clonal population arise principally from disturbances in the intracellular morphogenetic machinery that "builds" the cellular shape. The different ways in which evolutionary history may have affected the particulars of morphogenetic machineries in individual species, are similar to those demonstrated in other organisms (e.g., Monteiro et al. 2005, Marcil et al. 2006, Young & Badyaev 2006). Thus, we hypothesize that the different evolutionary history of several *Micrasterias* taxa may result not only in morphological differences but also in different patterns of morphological variation between individual species populations – and therefore in differences in shape depicted by the principal components of a PCA of morphometric data. Similarly, it was determined whether different discriminating signals were obtained in analyses of patterns of variation in separated polar lobes data as in datasets of complete semicells. The phylogenetic positions of our five *Micrasterias* species were analysed using 18S rDNA sequences. Firstly, this genetic data was compared with morphometric data in phenetic analyses using Kimura two-parameter genetic distances (Kimura 1980, Felsenstein 2004) of the polar lobes and complete semicells morphometric data of individual species. Secondly, the mutual phylogenetic affinities of *Micrasterias* species were analysed based on 18S rDNA. We did not specifically aim at a thorough phylogenetic study of the genus, but a basic insight into the evolutionary structure of the strains investigated in order to identify the morphometric markers corresponding to the individual clades. However, in order not to mix the phenetic data of geometric morphometrics (Adams et al. 2004) with cladistic reconstructions based on 18S rDNA sequences, formal comparisons of these data sets were not done. Thus, statistical analyses were limited to formal comparisons of phenetic indicators. Then, the relation of the morphometric indicators to the clades revealed by phylogenetic analysis is discussed.

Material and methods

Sampling

The species investigated were collected from the following localities: (1) benthos of flooded quarry pools near Cep village, S Bohemia, Czech Republic, col. 31. 10. 2005, pH 5.85 – *Micrasterias rotata* (strain deposited in Culture Collection of Charles University, Prague – CAUP K604) and *M. thomasiana* (strain CAUP K605); (2) benthos of a peat bog pool in "Borkovická Blata" Nature Reserve in S Bohemia, Czech Republic, col. 21. 5. 2006, pH 6.12 – *Micrasterias crux-melitensis* (strain CAUP K602), *M. truncata* (strain CAUP K606), *M. papillifera* (strain CAUP K603).

The strains were cultivated in liquid CAUP oligotrophic medium (Škaloud & Neustupa 2006) derived from BBM and DYIV culture media (Řezáčová 2006), at 23° C and illuminated at 40 μmol $m^{-2}s^{-1}$ using the light from 18W cool fluorescent tubes (Philips TLD 18W/33). The microphotographs were taken using an Olympus BX51 light microscope and Olympus Z5060 digital microphotographic equipment.

Geometric morphometrics

For each species, 50 randomly selected semicells were analysed and a total of 250 objects included in the geometric morphometric investigation. On each semicell, 21 structurally corresponding landmarks were delimited (Fig. 1), with 20 bilaterally symmetric landmarks and a single landmark positioned on the axis of symmetry. The positions of the landmarks were as follows: 1, 21 – margins of isthmus; 2, 20 – lower extremities of lower lateral lobules; 3, 19 – bases of incisions in lower lateral lobules; 4, 18 – upper extremities of lower lateral lobules; 5, 17 – bases of incisions between lateral lobules; 6, 16 – lower extremities of upper lateral lobules; 7, 15 – bases of incisions of upper lateral lobules; 8, 14 – upper extremities of upper lateral lobules; 9, 13 – bases of incisions between polar and lateral lobes; 10, 12 – lateral margins of the polar lobes; 11 – the central incision of the polar lobe. Landmarks were digitized in TpsDig, ver. 2.05. (Rohlf 2006) and the individual landmark configurations were superimposed by generalized Procrustes analysis (GPA) standardizing the size of the objects and optimizing their rotation and translation so that the distances between corresponding landmarks were minimized (Dryden & Mardia 1998, Zelditch et al. 2004, Slice 2005) in TpsRelw, ver. 1.42 (Rohlf 2005a). The TpsSmall, ver. 1.20. software (Rohlf 2003) was used to assess the correlation between Procrustes and the Kendall tangent space distances to ensure that the amount of shape variation in a data set was small enough to allow subsequent statistical analyses (see e.g., Rohlf 1998 or Zelditch et al. 2004 for details). As the correlation of Procrustes and the Kendall shape spaces was very high ($r = 0.999$), we proceeded with the morphometric analyses.

Cells of the genus *Micrasterias* are bilaterally symmetrical and, in addition, the anterior and posterior sides of a cell do not differ. Therefore, it is impossible to distinguish their respective left and right sides. Consequently, the two sides were symmetrized following the standard formula of Klingenberg et al. (2002). The symmetrization involved reflecting the cells (by multiplication of x-coordinates of all landmarks by –1), re-labelling of the bilaterally paired landmarks and averaging the original and mirrored configurations. The averages of original and reflected/relabelled cells are ideal symmetric shapes and each half, together with landmarks lying on axis of symmetry, bears all the information on the mor-

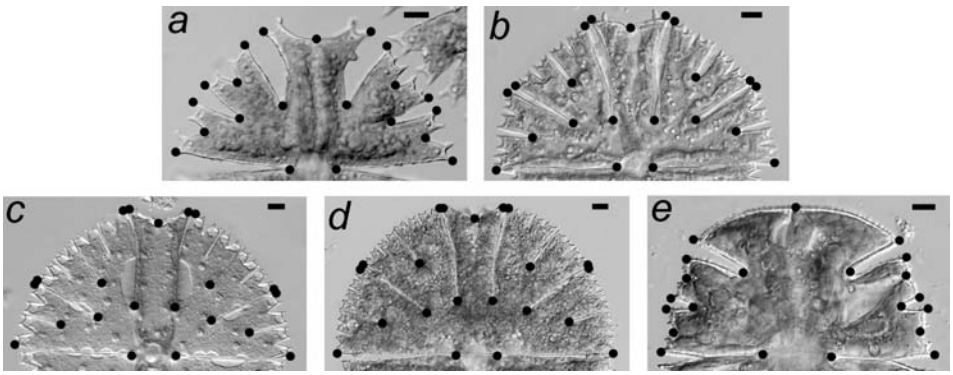

Fig. 1. – Figures of species investigated with positions of landmarks. a – *Micrasterias crux-melitensis*, strain CAUP K602, b – *M. papillifera*, strain CAUP K 603, c – *M. rotata*, strain CAUP K604, d – *M. thomasiana*, strain CAUP K605, e – *M. truncata*, strain CAUP K606. Bar = 10 μm.

phology of a symmetric object perceived by landmarks. Thus, further analysis of these symmetrized configurations omits the asymmetric component of the shape variation (Klingenberg et al. 2002, Neustupa & Hodač 2005). Using TpsRelw, we conducted the PCA of Procrustes coordinates (Zelditch et al. 2004). Marginal positions of morphospace depicted by the first three axes of PCA were illustrated as thin-plate splines (transformation grids) from consensus (average) shapes. Significance of shape differences between populations of each pair of investigated species (both complete semicells and isolated polar lobes data) was evaluated using permutation tests of Procrustes superimposed shape data (left halves of symmetric Procrustes superimposed configurations) on Wilk's λ and Goodall's F-ratio with 1000 permutations (Sheets et al. 2004, Gunz et al. 2005, Neustupa & Němcová 2007) in TpsRegr, ver. 1.31. (Rohlf 2005b). The position of individual species populations was illustrated by canonical variate analysis (CVA) of first ten axes of PCA that described 99.6% of total variability in data. CVA was performed in PAST, ver. 1.59. software (Hammer et al. 2001) and the 3-D ordination diagram was created in SigmaPlot, ver. 9.01.

The pattern of the shape change in subspaces described by PCA was analysed by evaluating the angle between hyperplanes (Zelditch et al. 2004). This method evaluates the difference in morphological subspaces spanned by a set of PC axes in two groups (Zelditch et al. 2006, Neustupa & Němcová 2007). PCA based on the Procrustes data was carried out independently for the two groups. We determined the angle between the (hyper-)planes defined by the first principal component and, in addition, by first three principal components of PCA in all five *Micrasterias* species. The IMP SpaceAngle program (Sheets 2002) was used for this analysis.

In a similar fashion, we conducted the analysis specifically aimed at the comparison of corresponding PC axes of principal component analyses (PCA) in two data sets with homologous landmark positions (Young & Badyaev 2006). Procrustes residuals characterize the vectors of displacement of each individual landmark of the given object from its position in average (consensus) configuration of the analysed set (Slice et al. 1998, Zelditch et

al. 2004). We compare the overall similarity in the shape change of two objects by evaluating the average angle between vectors defined by the displacements of all corresponding landmarks from the consensus configurations of each data set. The angle between two vectors is evaluated as

$$\theta = \arccos\left(\frac{a \cdot b}{|a| \cdot |b|}\right)$$

where *a* and *b* are vectors (Procrustes residuals) characterizing displacement of an individual landmark of the objects *A* and *B* from their position in average (consensus) configurations resulting from the generalized Procrustes analyses of their sets of objects (Arfken 1985, Young & Badyaev 2006). The mean angle α of angles θ, obtained from all corresponding landmark pairs, gives the measure of overall similarity in pattern of shape change between two objects depicted by landmark configurations. Smaller angle α indicates more similarity between patterns of variation in comparison to higher values of this measure. When measured in degrees, the theoretical maximum value of α is 180°, which indicates total dissimilarity in patterns of variation represented by displacement of landmarks in opposite directions. We took the extreme positions on first PC axis (describing the most important pattern of the shape variation in the data set) from separate PCAs of individual 50 cells in five investigated *Micrasterias* species. Note that while the angle between vectors is evaluated, the length of individual vectors (= landmark displacements) given by the score of actual configuration on the PC axis does not influence the results. We compared the corresponding positions of the first PC axes representing the single most important morphological trends in two species populations (retrieved from TpsRelw, ver. 1.42.) to arrive at the angle α by the method indicated above. As the sign of PC axes is arbitrary, we always took the pair of configurations with lower values of angle α, that represent more correlated (= corresponding) extremes of both PC axes. Consequently, the theoretical maximum of α taken as an average angle between corresponding positions of two PC axes is 90° (Young & Badyaev 2006). This value α gives us a measure of similarity between the shape change depicted by first PC axis in two morphospaces spanned by PCA of Procrustes aligned landmark data from 50 cells of two investigated species. The angle α could certainly further be used for more general comparisons of different PC axes or its significance evaluated by permutation tests, but this was outside the scope of this study. We used the routine in R 2.3.1. software (R Development Core Team 2006) to compute the angle α.

The structure of matrices of Procrustes distance (for shape differences between consensus configurations of individual species), angles between PC subspaces and average angles between vectors (for difference in patterns of variation) was illustrated using neighbour joining trees in PAST ver. 1.59. (Hammer et al. 2001). The correlations of individual morphometric matrices and the two-parameter Kimura distance (for difference in 18S rDNA) were evaluated using Mantel tests (Hollander & Wolfe 1999). Mantel tests with 10000 permutations were conducted in PAST, ver. 1.59. For analyses of variation in central parts of semicells, we chose the landmarks 8–14 (polar lobe and adjacent tips of upper lateral lobules) on all objects and conducted the same analyses as used for the complete landmarks configuration.

DNA extraction, amplification and sequencing

After centrifugation, algal cells were mechanically disrupted by shaking in the presence of glass beads (0.5 mm diameter, Sigma). Genomic DNA was extracted using the Invisorb Spin Plant Mini Kit (Invitek) following the instructions given by the manufacturer. 18S rDNA was amplified by polymerase chain reaction (PCR) using eukaryotic general primers
34F (5´-GTCTCAAAGATTAAGCCATGC-3´) and
18L (5´-CACCTACGGAAACCTTGTTACGACTT-3´).
PCR reactions were performed in a 50 µl reaction volume containing a reaction mix of 0.2 mM of each of the four dNTPs, 2 mM $MgCl_2$, 4% DMSO, 0.2 mM of each PCR primer, 1–3 µl DNA template and 1 unit Taq polymerase with the supplier's buffer (BIOTAQ, Bioline). After an initial denaturing step at 95 °C for 5 min, 35 cycles of a denaturing at 94 °C for 40 s, annealing at 51 °C for 40 s and elongation at 72 °C for 2 min were performed, followed by a final extension at 72 °C for 10 min. The PCR products were cleaned using the Invisorb Spin PCRapid Kit (Invitek) and quantified on 1% agarose gel. The purified amplification products were sequenced with a set of sequencing primers (Hamby et al. 1988) using the protocol for the DNA sequencing kit (ABI Prism Big-Dye terminator cycle sequencing ready reaction, Applied BioSystems). Purified sequencing reactions were run on 3100-Avant Genetic Analyzer (Applied Biosystems). Sequencing reads were assembled and edited using SeqAssem (SequentiX Software). Newly obtained sequences were deposited in EMBL Nucleotide Sequence Database (for accession numbers see Fig. 6).

Sequence alignment and phylogenetic analyses

After initial automatic alignment using ClustalX 1.83 (Thompson et al. 1997), the sequences were manually aligned with two 18S rDNA sequences of the genus *Micrasterias* deposited in the NCBI (National Center for Biotechnology Information) using MEGA 3.1 (Kumar et al. 2004). Ambiguously aligned regions and positions with deletions in most sequences were removed from the alignment, resulting in an alignment comprising 1721 base positions. Evolutionary model (for ML and NJ analyses) was selected via Modeltest version 3.7 (Posada & Crandall 1998). To obtain a larger data set for the estimation, additional 35 selected sequences of the *Zygnemophyceae* were added to the alignment. The alignment is deposited in the EMBL-Align database (http://www.ebi.ac.uk/embl/Submission/alignment.html; no. ALIGN_001114). The model selected by the hierarchical likelihood ratio test (hLRT) was the Tamura-Nei model (TrN) with the proportion of invariable sites (I) and the rate heterogeneity among sites following a gamma (Γ) distribution. Phylogenetic trees were inferred from the aligned sequence data by the neighbour-joining (NJ), maximum parsimony (MP) and maximum likelihood (ML) methods using PAUP* 4.0b10 (Swofford 2003). In all methods, heuristic bootstrap analyses with 1000 (NJ, MP) or 100 replicates (ML) were conducted. MP phylogenies were constructed using the exhaustive search option. The tree searches for ML analyses were conducted heuristically using the tree-bisection-reconnection (TBR) branch-swapping algorithm. Starting trees were obtained via neighbour-joining method. Bayesian analysis was conducted using MrBayes 3.1 (Ronquist & Huelsenbeck 2003). As the TrN model is not available in MrBayes, we used the general time-reversible model (GTR + I + Γ) instead. Six parallel MCMC runs were carried out for two million generations, sampling every 100 generations for a total of 20,000 samples. The first 400 samples were discarded as "burn-in" and posterior probabil-

ities of the branching pattern were calculated on the basis of the consensus of the remaining trees.

Results

The proportion of variation described by the first three axes of separate principal component analyses of five *Micrasterias* species and corresponding shape changes are illustrated in Table 1 and Fig. 2. The first principal component of the analysis of three species (*M. papillifera*, *M. rotata*, *M. thomasiana*) described primarily the widening of the polar lobe connected with the tendency to more shallow incisions between individual lobes and lobules in cells with wide polar lobes. In *Micrasterias truncata* and *M. crux-melitensis*, this morphological trend was less conspicuous on the first PC axis. On the other hand, there was a clear shape change characterized by a distinct widening/narrowing of the incision between polar and lateral lobes in both of these species. The second PC axis was characterized by a conspicuous trend in the widening/narrowing of lower lateral lobule in all five species. However, there were other minute morphological trends on the second axis that were different in individual species. The third axis described a similar morphological trend in *Micrasterias papilifera*, *M. rotata* and *M. thomasiana*, emphasizing the width proportions of two main lateral lobules. In *Micrasterias crux-melitensis* there was a clear tendency in the widening/narrowing of the polar lobe. In *Micrasterias truncata*, this axis described variation in the overall stretching/shortening of the semicells.

Canonical variate analysis (CVA) of five species based on the scores of the 250 complete semicells on the first ten PC axes revealed highly significant differences between species (Wilks $\lambda = 9.275.10^{-7}$, $P = 0$). The positions of individual groups on the first three CV axes (Fig. 3) illustrated clear delimitation of individual species on the basis of landmark-based shape data. The shape differences between pairs of species were evaluated by permutation tests of shape data. The tests demonstrated significant differences in all species pairs with permutation P-values = 0.001, both in complete configurations and isolated polar lobe data sets. The highest values of Wilks λ (and, correspondingly, the lowest Goodall's F-ratios) between *Micrasterias papillifera*, *M. rotata* and *M. thomasiana* indicate that they are similar in shape – again both in complete semicells and isolated polar lobes. On the other hand, *Micrasterias crux-melitensis* and *M. truncata* were unlike the other species. The shape of *Micrasterias truncata* is very different from that of the other species, consistently in data sets of complete semicells as well as isolated polar lobes (Table 2).

The analyses of patterns of variation spanned by PCA axes revealed differences between individual morphometric distance measures, as well as between data sets of complete semicells and polar lobes (Table 3, Figs 4, 5). When using Procrustes distance as a distance measure, the topology indicating dissimilarity of *M. truncata* was consistent both in complete semicells and polar lobes (Fig. 5a, b). The angles between subspaces spanned by the first PC axis (sensu Zelditch et al. 2004) gave a somewhat similar picture (Fig. 5c, d) and did not clearly demonstrate that the narrow-lobed species *M. papillifera, M. rotata* and *M. thomasiana* were similar in variation structure. In analyses of angles between subspaces of first three PC axes, variation in population of *Micrasterias truncata* was also clearly different from all of the other species. On the other hand, *Micrasterias papillifera, M. rotata* and *M. thomasiana* were similar (Table 3, Fig. 5e, f). However, the average angles between vec-

Table 1. – The singular values and percentages of variability explained for first, second and third axes in PCA of five *Micrasterias* species populations.

Species	PC1		PC2		PC3	
	Singular value	% explained	Singular value	% explained	Singular value	% explained
M. crux-melitensis	0.164	45.07	0.099	16.68	0.089	13.19
M. papillifera	0.126	49.98	0.061	11.50	0.054	9.18
M. rotata	0.168	49.78	0.114	23.02	0.061	6.62
M. thomasiana	0.117	40.46	0.084	20.75	0.057	9.63
M. truncata	0.119	38.21	0.087	20.29	0.067	11.99

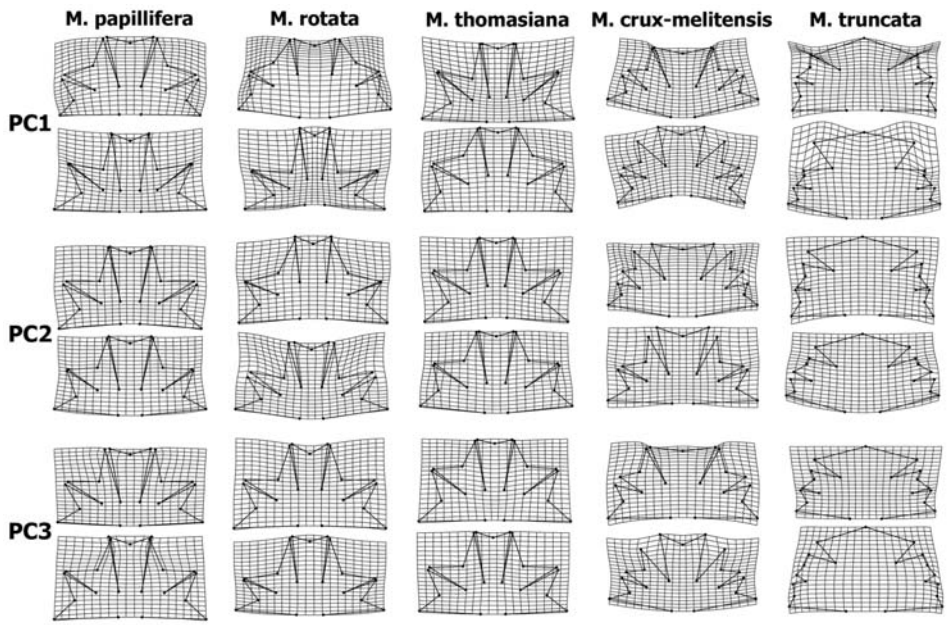

Fig. 2. – Transformation grids from consensus configurations of extreme positions on first three PC axes of five *Micrasterias* species. The deformations were magnified twice in order to better illustrate the shape changes.

tors of landmark displacements characteristic for the first PC axes in each pair of species revealed a different pattern. *Micrasterias papillifera, M. rotata* and *M. thomasiana* formed a closely related group and *Micrasterias crux-melitensis* with *M. truncata* were also more related to each other than to the remaining species (Figs 4, 5). This pattern was more pronounced in polar lobe data than that for complete semicells (Figs 4, 5g, h).

The Mantel tests of matrix correlations in phenetic data (Kimura two-parameter distances in 18S rDNA sequences and morphometric indicators) demonstrated generally positive correlations between genetic distances and shape characteristics (Table 4). The analyses revealed that the morphological variation of polar lobes accords with the genetic data. On the other hand, patterns of variation of complete semicell configurations and the Procrustes distances between pairs of species (indicating their morphological similarity) were less correlated with 18S rDNA genetic distances (Table 4). Maximum likelihood and

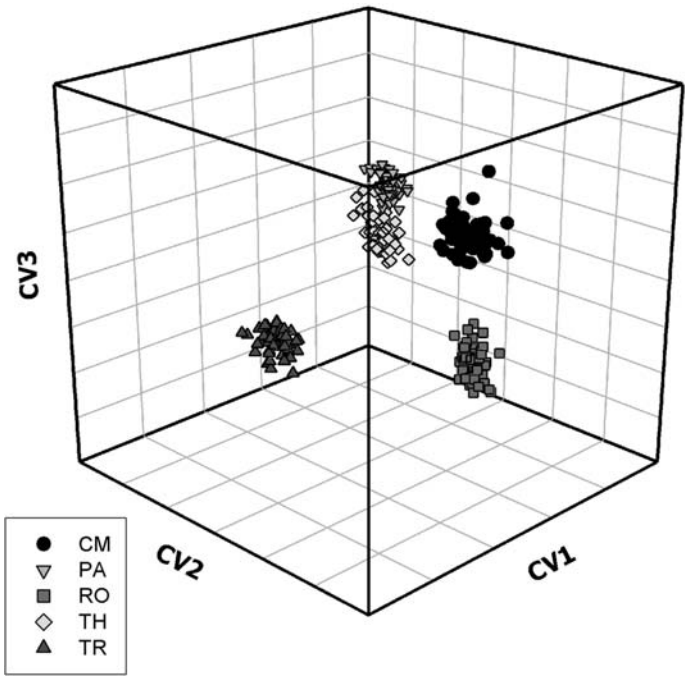

Fig. 3. – The ordination diagram of first three CV axes discriminating the *Micrasterias* species groups based on geometric morphometric shape data of complete semicells. CM = *Micrasterias crux-melitensis*; PA = *M. papillifera*; RO = *M. rotata*; TH = *M. thomasiana*; TR = *M. truncata*.

Table 2. –The indicators of group shape differences of *Micrasterias* species. In each species pair, the first line indicates Procrustes distances, the second Wilk's λ and the third the Goodall's F-ratio (in complete configurations and isolated polar lobes separated by slash in all lines).

	M. papillifera	*M. rotata*	*M. thomasiana*	*M. truncata*
	0.177 / 0.408	0.175 / 0.370	0.206 / 0.451	0.224 / 0.426
M. crux-melitensis	0.008 / 0.017	0.009 / 0.032	0.004 / 0.012	0.005 / 0.007
	650.5 / 1363.0	539.3 / 921.3	723.7 / 1706.8	932.1 / 1455.2
		0.080 / 0.082	0.053 / 0.053	0.382 / 0.791
M. papillifera		0.011 / 0.514	0.032 / 0.297	0.002 / 0.002
		243.9 / 21.9	92.2 / 63.8	3142.2 / 7478.5
			0.080 / 0.112	0.371 / 0.752
M. rotata			0.021 / 0.207	0.002 / 0.003
			186.8 / 97.8	2435.5 / 5577.5
				0.0409 / 0.804
M. thomasiana				0.001 / 0.001
				3157.7 / 8884.7

Bayesian analyses of the molecular data recovered identical topologies, differentiating the *Micrasterias* species into two clades (Fig. 6). The differentiation was well supported in bootstrap and credibility tests using the NJ, ML, MP (100%) and MrBayes (1.0) methods.

Table 3. – Values of individual distance measures of similarities in patterns of variation in pairs of species populations. The order of the values is indicated in the upper left cell. AS–1PC = angles between subspaces (1 PC axis); AS–3PC = angles between subspaces (3 PC axis); AV = angles between vectors of corresponding landmarks on first PC axis.

Complete configurations: – AS-1PC / AS-3PC / AV polar lobes: – AS-1PC / AS-3PC / AV	*M. papillifera*	*M. rotata*	*M. thomasiana*	*M. truncata*
M. crux-melitensis	57.7 / 72.4 / 84.8 56.1 / 40.1 / 81.3	78.9 / 81.3 / 83.4 66.6 / 62.7 / 89.5	63.9 / 92.4 / 72.4 69.6 / 75.5 / 87.5	75.6 / 103.0 / 83.7 44.7 / 84.0 / 43.0
M. papillifera		57.1 / 71.7 / 66.2 27.5 / 56.0 / 11.8	24.3 / 77.6 / 30.3 22.6 / 57.7 / 15.0	85.4 / 105.5 / 81.2 87.0 / 95.8 / 68.6
M. rotata			56.3 / 60.0 / 52.0 20.3 / 57.7 / 14.0	86.2 / 107.8 / 78.8 87.9 / 114.1 / 81.0
M. thomasiana				89.5 / 113.1 / 81.8 85.8 / 108.0 / 87.2

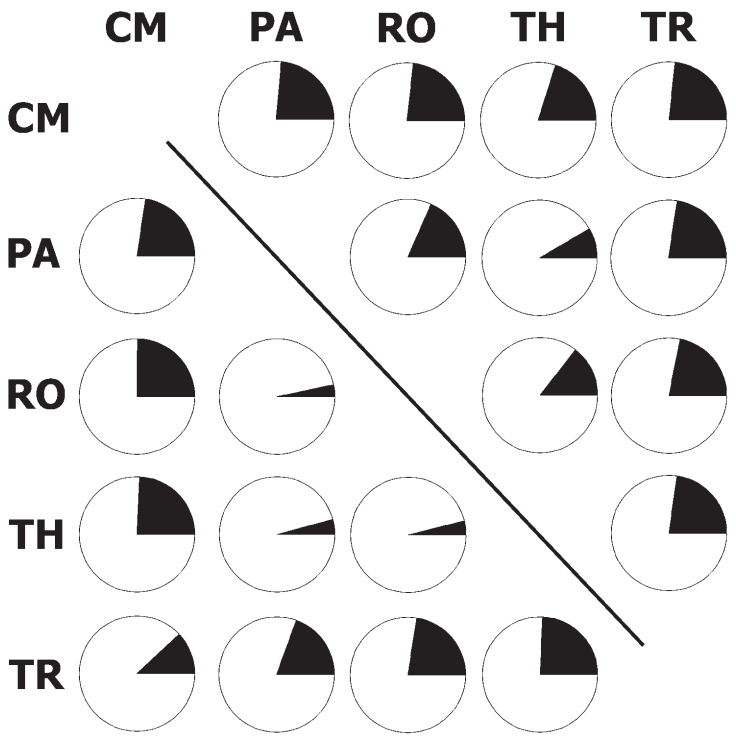

Fig. 4. – The average angles of vectors defined by landmark positions from consensus configurations on the first PC axis of pairs of species. Angles in complete semicell configurations are illustrated in upper triangle, the angles in polar lobes in lower triangle. The numeric values of angles are given in Table 3. Note the difference in *M. crux-melitensis* vs *M. truncata* angle between both data sets. For abbreviations see Fig. 3.

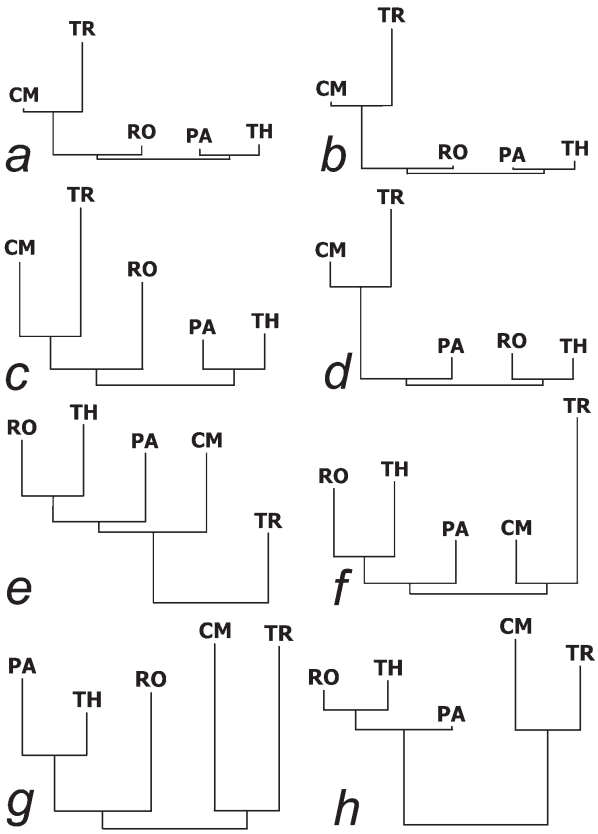

Fig. 5. – Neighbour joining trees of different morphometric distance measures. For species abbreviations see Fig. 3. a – Procrustes distances, complete semicells, b – Procrustes distances, polar lobes, c – angles between subspaces, 1 PC, complete semicells, d – angles between subspaces, 1 PC, polar lobes, e – angles between subspaces, 3 PC, complete semicells, f – angles between subspaces, 3 PC, polar lobes, g – average angles of landmark vectors on first PC, complete semicells, h – average angles of landmark vectors on first PC, polar lobes.

Table 4. – Results of Mantel tests of matrix correlations. Significant correlations are marked with asterisk (*). GD = Kimura two-parameter genetic distances; PD = Procrustes morphometric distances; AS–1PC = angles between subspaces (1 PC axis); AS–3PC = angles between subspaces (3 PC axis); AV = angles between vectors of corresponding landmarks on first PC axis.

	Matrix correlation coefficient (r)	Rank of the original matrix among 120 possible permutations
GD × PD (complete configurations)	0.4761	7
GD × PD (polar lobes)	0.5559	7
GD × AS–1PC (complete configurations)	0.4858	7
GD × AS–1PC (polar lobes)	0.7370 *	5
GD × AS–3PC (complete configurations)	0.2216	21
GD × AS–3PC (polar lobes)	0.1828	21
GD × AV (complete configurations)	0.5282 *	6
GD × AV (polar lobes)	0.8661 *	1

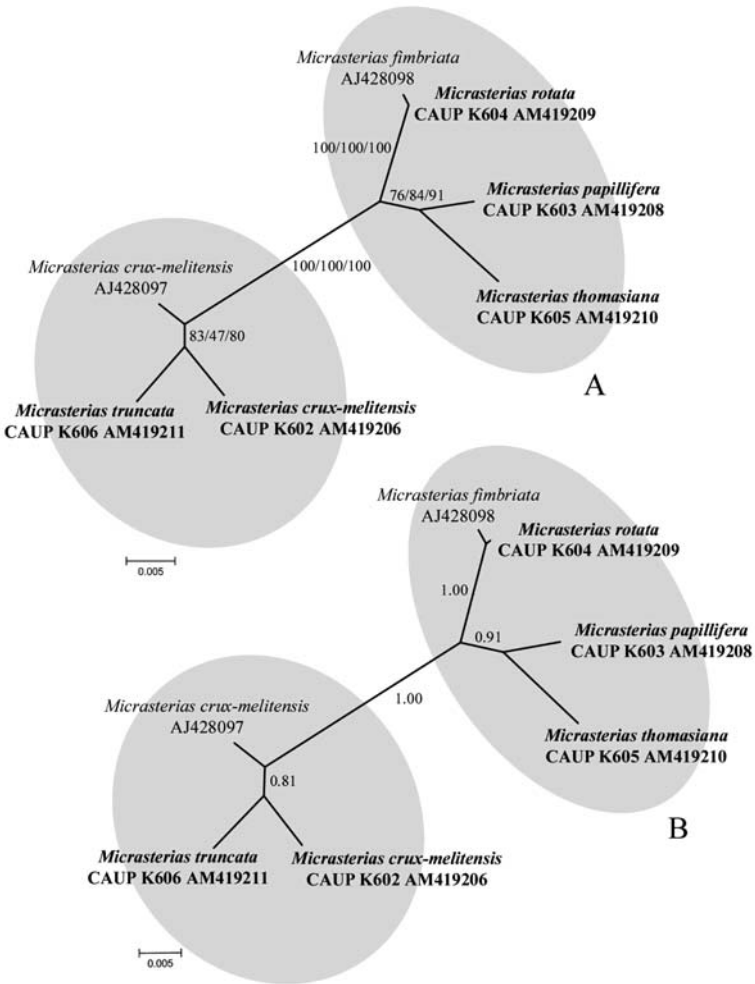

Fig. 6. – Maximum likelihood (A) and Bayesian (B) trees resulting from analyses of 18S rDNA sequences. ML/MP/NJ bootstrap scores (A) and Bayesian posterior probabilities (B) are provided for each node. New 18S rDNA sequences obtained in this study are indicated in bold.

Species with a wide polar lobe (*M. crux-melitensis* and *M. truncata*) clustered together. However, two sequences of *M. crux-melitensis* (sequence AJ428097 based on strain NIES 152 and sequence AM419206, strain CAUP K602) differed by 21 nucleotide positions and so probably this species is not a single taxon. In this respect, we should note that the correct identification of strain NIES 152, whose sequence was originally published by Gontcharov et al. (2003), was confirmed by the microphotographs published on the official web site of NIES (http://www.nies.go.jp/biology/mcc/home.htm). The second clade was composed of species with narrow polar lobe. *Micrasterias rotata* and *M. fimbriata* clustered into a highly supported clade sister to a one formed by *Micrasterias papillifera* and *M. thomasiana*.

Discussion

In accordance with a previous geometric morphometric study of *Micrasterias* (Neustupa & Šťastný 2006), complete semicell configurations as well as the isolated polar lobe data clearly differentiated individual species. According to the shape data (Procrustes distances) *Micrasterias crux-melitensis* and *M. truncata* form a loosely connected group, dissimilar from the other three species with narrow polar lobes and deep incision between lateral lobules (*M. papillifera, M. rotata* and *M. thomasiana*) (Fig. 5a, b). Thus, comparing the Procrustes distances, the morphometric signal from data of complete semicells and isolated polar lobes was similar. However, in analyses of patterns of variation, the differences between complete semicells and isolated polar lobes were considerable (Fig. 4). The pattern described by the first axis in PCA of five species populations indicated grouping of *Micrasterias crux-melitensis* and *M. truncata* (Fig. 5c, d, g, h). However, the sister group composed of the three other species was consistently differentiated in neighbour joining phenograms based on average angles between vectors of displacements in corresponding landmarks on the first PC axis (Fig. 5g, h). A similar pattern was also revealed by an analysis of the angle between the hyperplanes spanned by the first three PC axes of isolated polar lobes data (Fig. 5f). Parallel analysis of complete semicells, however, did not accord with this topology (Fig. 5e).

There were clearly higher correlations of 18S rDNA genetic distances with morphometric data extracted from polar lobes than from complete semicells. In general, these results confirm the traditional taxonomic opinion (Prescott et al. 1977, Růžička 1981, Coesel 1985, Lenzenweger 1996). Thus, the structure and variation of polar lobes truly appears to be the most useful morphological marker for *Micrasterias* taxonomy. The patterns of variation in polar lobes (plus adjacent extremities of upper lateral lobules) on the first PC axis correlated most strongly with the genetic distance data (Table 4). At the same time, the distances between individual species in terms of this indicator corresponded well with the phylogenetic affinities reconstructed from the 18S rDNA data. In this respect, the analyses of patterns of variation in populations were more informative than the comparisons of morphology. For example, Procrustes distance of mean semicell shapes, reflecting the difference in actual morphology of cells, was 0.224 between *M. crux-melitensis* and *M. truncata* – a pair of phylogenetically closely related species. In comparison, the Procrustes distance between the non-monophyletic pair, *M. crux-melitensis* and *M. rotata*, was only 0.175 and that between *M. crux-melitensis* and *M. papillifera*, 0.177. However, the average angles between vectors of polar lobe configurations were only 42.96° between *M. crux-melitensis* and *M. truncata*, but 89.59° between *M. crux-melitensis* and *M. rotata*, and 81.34° between *M. crux-melitensis* and *M. papillifera* (Table 3, Fig. 4). Thus, the average angle between vectors of landmark displacement in two configurations on the first PC axis appeared to be the most useful measure for the phenetic comparison of *Micrasterias* phenotypic and molecular data. It unambiguously grouped even the morphologically dissimilar but phylogenetically related *M. crux-melitensis* and *M. truncata*. On the other hand, morphological difference alone (measured as Procrustes distance) was useful at the level of clades, but probably not as powerful at the species level. This is even more evident when considering the probable pseudocryptic diversity within the group (see below, Blackburn & Tyler 1981, 1987). Thus, the analyses of variation patterns, applied to polar lobe configurations, appear to be

a most useful protocol for future comparisons of phylogeny and morphology in desmids. We propose that morphometric analyses should focus principally on central parts of semicells – polar lobes and adjacent parts of lateral lobes. Of course, the availability of homologous landmarks is crucial for any such analysis. In this respect, analyses involving not only fixed landmarks but also semilandmarks that delimit outlines of curves of structures (Bookstein 1997, Neustupa & Hodač 2005, Neustupa & Němcová 2007, Sheets et al. 2004) should be especially useful for retrieving the phylogeny-correlated morphometric signal. As the analyses of patterns of variation do not directly depend on actual morphological differences, they could reveal the species-specific differences in morphologically similar or even cryptic lineages – e.g., the *Micrasterias crux-melitensis* complex, which possibly includes phylogenetically differentiated cryptic or pseudocryptic taxa. In this respect, morphometric analyses of actual shape difference, including those presented in this study, clearly could have a weaker discriminative power than analyses of the patterns of variation.

On the other hand, similarities in patterns of variation can nonetheless be useful for investigating phenotypic correlations in morphologically heterogeneous complexes. In this respect, we believe that this approach could be used in botanical studies of complex and plastic structures, such as flowers of vascular plants (Gómez et al. 2006, Shipunov & Bateman 2005, Těšitel & Štěch 2007), *Halimeda* segments (Verbruggen et al. 2005a, 2005b) or green unicellular algae (Neustupa 2004, 2005).

The phylogenetic analyses revealed a consistent two-clade pattern in the *Micrasterias* species investigated (Fig. 6). The differentiation of species with broad polar lobes (*Micrasterias crux-melitensis* / *M. truncata*) from those with narrow polar lobes corresponds with the clustering pattern in a geometric morphometric analysis of 14 *Micrasterias* species from Central Europe (Neustupa & Šťastný 2006). Gontcharov et al. (2003) confirmed the phylogenetic position of *Micrasterias* within the *Desmidiaceae*, but indicated that this genus is possibly paraphyletic. Similar non-monophyletic status of other traditional desmid genera (e.g. in *Cosmarium*, *Staurastrum*, *Staurodesmus* and *Xanthidium*) was demonstrated by Gontcharov et al. (2003) and Gontcharov & Melkonian (2005). The aim of this study was not to determine the generic position of *Micrasterias* within the *Desmidiaceae*, which should be based on a broader phylogenetic analysis and more extensive sequence data. In our phylogenetic analyses, *Micrasterias rotata* was placed in a lineage closely related to *M. fimbriata*, a morphologically similar species with a narrow polar lobe and deeply divided lateral lobes, and they were placed into a clade of generally narrow-lobed species. Two sequences belonging to *Micrasterias crux-melitensis* differed by 21 nucleotide positions and did not form a common lineage. This divergence demonstrates the possible existence of cryptic species within *Desmidiaceae*, which might be crucial for the future evaluation of the current desmid species concept based on morphological characters. Infraspecific differentiation coupled with reproductive isolation was revealed in *Micrasterias thomasiana* (Blackburn & Tyler 1981, 1987). The evidence of phylogenetic divergence based on molecular data and morphometric differentiation of individual strains could lead to a future revision of the species concept in such widely distributed and variable desmid taxa as *M. crux-melitensis* or *M. thomasiana*. Phenotypic analyses based on patterns of variation could be more successful in delimiting such morphologically very similar complexes than the analyses of morphology.

Acknowledgements

This study was supported by grant no. 206/05/P139 of Czech Science Foundation and by the research project of the Czech Ministry of Education no. 0021620828. We thank anonymous reviewers for their comments, which led us to improve the manuscript. Tony Dixon kindly improved our English.

Souhrn

V této studii jsme provedli geometricko-morfometrické analýzy klonálních populací v kulturách u pěti druhů rodu *Micrasterias* (*M. crux-melitensis*, *M. papillifera*, *M. rotata*, *M. thomasiana*, *M. truncata*). Pomocí metod srovnávání tvaroprostorů definovaných osami PCA populačních vzorků jsme analyzovali kvalitativní strukturu morfologické plasticity. Dále jsme provedli analýzy sekvencí 18S rDNA. Fenetická srovnání ukázala všeobecně pozitivní vysokou korelaci různých morfometrických ukazatelů získaných z polárních laloků buněk s genetickými vzdálenostmi. Morfometrická data získaná z kompletních polobuněk byla s genetickými ukazately zřetelně méně korelovaná. Fylogenetická analýza ukázala pravděpodobnou evoluční strukturu rodu sestávajícího ze dvou linií, kterým nejlépe odpovídají zjištěné kvalitativní parametry populační morfologické variability u polárních laloků buněk. V diskusi navrhujeme, že právě tento ukazatel – tedy struktura variability polárních laloků – by měl být do budoucnosti používán při fenotypových analýzách morfologicky velmi podobných nebo kryptických druhů této skupiny.

References

Adams D. C., Rohlf F. J. & Slice D. E. (2004): Geometric morphometrics: ten years of progress following the 'revolution'. – Ital. J. Zool. 71: 5–16.

Arfken G. (1985): Scalar or dot product. – In: Orlando F. L. (ed.), Mathematical methods for physicists, p. 1–18, Academic Press, London.

Beszteri B., Ács E. & Medlin L. (2005): Conventional and geometric morphometric studies of valve ultrastructural variation in two closely related *Cyclotella* species (*Bacillariophyta*). – Eur. J. Phycol. 40: 89–103.

Bicudo C. E. M. & Gil-Gil F. (2003): Different morphological expressions or taxonomical entities of *Micrasterias arcuata* (*Desmidiales, Zygnemaphyceae*)? – Biologia 58: 645–655.

Blackburn S. I. & Tyler P. A. (1981): Sexual reproduction in desmids with special reference to *Micrasterias thomasiana* var. *notata* (Nordst.) Gronblad. – Br. Phyc. J. 16: 217–229.

Blackburn S. I. & Tyler P. A. (1987): On the nature of eclectic species – a tiered approach to genetic compatibility in the desmid *Micrasterias thomasiana*. – Br. Phyc J. 22: 277–298.

Bookstein F. L. (1997): Landmark methods for forms without landmarks: morphometrics of group differences in outline shape. – Med. Image. Anal. 1: 225–243.

Coesel P. F. M. (1985): De Desmidiaceeën van Nederland. 3. – Wetensch. Meded. K. N. N. V., Utrecht.

Dryden I. L. & Mardia K. V. (1998): Statistical shape analysis. – John Wiley & Sons, New York.

Felsenstein J. (2004): Inferring phylogenies. – Sinauer Ass. Inc., Sunderland.

Gil-Gil F. & Bicudo C. E. M. (2000): Ecology of *Micrasterias arcuata* var. *arcuata* and *M. arcuata* var. *expansa* (*Desmidiaceae*, *Zygnemaphyceae*) in the Açude do Jacaré, state of Sao Paulo, southern Brazil. – Algol. Stud. 98: 71–89.

Gomez J. M., Perfectti F. & Camacho J. P. M. (2006): Natural selection on *Erysimum mediohispanicum* flower shape: insights into the evolution of zygomorphy. – Am. Nat. 168: 531–545.

Gontcharov A. A., Marin B. & Melkonian M. (2003): Molecular phylogeny of conjugating green algae (*Zygnemophyceae*, *Streptophyta*) inferred from SSU rDNA sequence comparisons. – J. Mol. Evol. 56: 89–104.

Gontcharov A. A. & Melkonian M. (2005): Molecular phylogeny of *Staurastrum* Meyen ex Ralfs and related genera (*Zygnematophyceae*, *Streptophyta*) based on coding and noncoding rDNA sequence comparisons. – J. Phycol. 41: 887–899.

Gunz P., Mitteroecker P. & Bookstein F L. (2005): Semilandmarks in three dimensions. – In: Slice D. E. (ed.), Modern morphometrics in physical anthropology, p. 73–98, Kluwer Acad/Plenum Publ, New York.

Haines A. J. & Crampton J. S. (2000): Improvements to the method of Fourier shape analysis as applied in morphometric studies. – Palaeontology 43: 765–783.

Hamby R. K., Sim L. E., Issel L. E. & Zimmer E. A. (1988): Direct RNA sequencing: optimization of extraction and sequencing techniques for work with higher plants. – Pl. Mol. Biol. Rep. 6: 179–197.

Hammer Ø., Harper D.A.T. & Ryan P. D. (2001): PAST: Paleontological Statistics Software Package for Education and Data Analysis. – Palaeont. Electr. 4 (1): 9pp.

Hollander M. & Wolfe D. A. (1999): Nonparametric statistical methods. – Wiley Interscience, New York.

Kimura M. (1980): A simple method for estimating evolutionary rates of base substitutions through comparative studies of nucleotide sequences. – J. Mol. Evol. 16: 111–120.

Klingenberg C. P., Barluenga M. & Meyer A. (2002): Shape analysis of symmetric structures: quantifying variation among individuals and asymmetry. – Evolution 56: 1909–1920.

Kumar S., Tamura K. & Nei M. (2004): MEGA3: Integrated software for Molecular Evolutionary Genetics Analysis and sequence alignment. – Brief. Bioinform. 5: 150–163.

Lenzenweger R. (1996): Desmidiaceenflora von Österreich, Teil 1. – J. Cramer Verl., Berlin.

Marcil J., Swain D. P. & Hutchings J. A. (2006): Genetic and environmental components of phenotypic variation in body shape among populations of Atlantic cod (*Gadus morhua* L.). – Biol. J. Linn. Soc. 88: 351–365

Monteiro L. R., Bonato V. & dos Reis S. F. (2005): Evolutionary integration and morphological diversification in complex morphological structures: mandible shape divergence in spiny rats (*Rodentia*, *Echimyidae*). – Evol. Dev. 7: 429–439.

Neustupa J. (2004): Two new aerophytic species of the genus *Podohedra* Düringer (*Chlorophyceae*) – Algol. Stud. 112: 1–16.

Neustupa J. (2005): Phenotypic plasticity of microalgal cultures in culture collections: a geometric morphometric appproach. – Oceanol. Hydrobiol. Stud. 34: 97–107.

Neustupa J. & Hodač L. (2005): Changes in shape of the coenobial cells of an experimental strain of *Pediastrum duplex* var. *duplex* (*Chlorophyta*) reared at different pHs. – Preslia 77: 439–452.

Neustupa J. & Němcová Y. (2007): A geometric morphometric study of the variation in scales of *Mallomonas striata* (*Synurophyceae*, *Heterokontophyta*). – Phycologia 46: 123–130**.**

Neustupa J. & Šťastný J. (2006): The geometric morphometric study of Central European species of the genus *Micrasterias* (*Zygnematophyceae*, *Viridiplantae*). – Preslia 78: 253–263.

Posada D. & Crandall K. A. (1998): Modeltest: testing the model of DNA substitution. – Bioinformatics 14: 817–818.

Prescott G. W., Croasdale H. T. & Vinyard W. C. (1977): A synopsis of North American desmids, Part II. *Desmidiaceae*: *Placodermae*, Section 2. – Univ. Nebraska Press, Lincoln.

Quillevere F., Debat V. & Auffray J. C. (2002): Ontogenetic and evolutionary patterns of shape differentiation during the initial diversification of Paleocene acarininids (planktonic foraminifera). – Paleobiology 28: 435–448.

Ralfs J. (1848): The British *Desmidieae*. – Reeve, Benham and Reeve, London.

R Development Core Team (2006) R: A language and environment for statistical computing. – R Foundation for Statistical Computing, Vienna.

Řezáčová M. (2006): *Mallomonas kalinae* (*Synurophyceae*), a new species of alga from northern Bohemia, Czech Republic. – Preslia 78: 353–358.

Rohlf F. J. (1998): On application of geometric morphometrics to studies of ontogeny and phylogeny. – Syst. Biol. 47: 147–158.

Rohlf F. J. (2003): TpsSmall Version 1.20. – Department of Ecology and Evolution, State University of New York at Stony Brook, New York.

Rohlf F. J. (2005a): TpsRelw Version 1.42. – Department of Ecology and Evolution, State University of New York at Stony Brook, New York.

Rohlf F. J. (2005b): TpsRegr Version 1.31. – Department of Ecology and Evolution, State University of New York at Stony Brook, New York.

Rohlf F. J. (2006): TpsDig Version 2.05. – Department of Ecology and Evolution, State University of New York at Stony Brook, New York.

Ronquist F. & Huelsenbeck J. P. (2003): MRBAYES 3: Bayesian phylogenetic inference under mixed models. – Bioinformatics 19: 1572–1574.

Růžička J. (1981): Die Desmidiaceen Mitteleuropas, Band 1, 2. Lieferung. – E. Schweizerbart´sche Verl., Stuttgart.

Sheets D. H. (2002): IMP: Integrated Morphometrics Package. – Department of Physics, Canisius College, Buffalo.

Sheets D. H., Kim K. & Mitchell C. E. (2004): A combined landmark and outline-based approach to ontogenetic shape change in the Ordovician trilobite *Triarthrus becki*. – In: Elewa A. M. T. (ed.), Morphometrics. Applications in biology and paleontology, p. 67–82, Springer Verlag, Berlin.

Shipunov A B. & Bateman R. M. (2005): Geometric morphometrics as a tool for understanding *Dactylorhiza* (*Orchidaceae*) diversity in European Russia. – Biol. J. Linn. Soc. 85: 1–12.

Slice D. E. (2005): Modern morphometrics. – In: Slice D. E. (ed.), Modern morphometrics in physical anthropology, p. 1–46, Kluwer Acad/Plenum Publ, New York.

Slice D. E., Bookstein F. L., Marcus L. F. & Rohlf F. J. (1998): A glossary for geometric morphometrics. – State University of New York, New York.

Swofford D. L. (2003): PAUP*. Phylogenetic analysis using parsimony (and other methods). Version 4. – Sinauer Ass. Inc., Sunderland.

Škaloud P. & Neustupa J. (2006): CAUP – The culture collection of algae of Charles University of Prague. – Dept. Botany, Charles Univ., Prague.

Těšitel J. & Štech M. (2007): Morphological variation in the *Melampyrum sylvaticum* group within the transitional zone between *M. sylvaticum* s. str. and *M. herbichii*. – Preslia 79: 83–99.

Thompson J. D., Gibson T. J., Plewniak F., Jeanmougin F. & Higgins D. G. (1997): The ClustalX windows interface: flexible strategies for multiple sequence alignment aided by quality analysis tools. – Nucl. Acid. Res. 25: 4876–4882.

Verbruggen H., De Clerck O., Cocquyt E., Kooistra W. H. C. F. & Coppejans E. (2005): Morphometric taxonomy of siphonous green algae: A methodological study within the genus *Halimeda* (*Bryopsidales*). – J. Phycol. 41: 126–139.

Verbruggen H., De Clerck O., Kooistra W. H. C. F. & Coppejans E. (2005): Molecular and morphometric data pinpoint species boundaries in *Halimeda* section *Rhipsalis* (*Bryopsidales*, *Chlorophyta*). – J. Phycol. 41: 606–621.

Vyverman W. & Viane R. (1995): Morphological variation along an altitudinal gradient in the *Micrasterias cruxmelitensis – M. radians* complex (*Algae*, *Zygnemaphyceae*, *Desmidiales*) from Papua New Guinea. – Nova Hedwigia 60: 187–197.

Young R. L. & Badyaev A. V. (2006): Evolutionary persistence of phenotypic integration: influence of developmental and functional relationships on complex trait evolution. – Evolution 60: 1291–1299.

Zelditch M. L., Swiderski D. L., Sheets D. H. & Fink W. L. (2004): Geometric morphometrics for biologists: a primer. – Elsevier Academic Press, London.

Zelditch M. L., Mezey J., Sheets D. H., Lundrigan B. L. & Garland T. (2006): Developmental regulation of skull morphology II. Ontogenetic dynamics of covariance. – Evolution & Development 8: 46–60.

Received 4 May 2007
Revision received 19 July 2007
Accepted 29 July 2007